SOCIETY FOR EXPERIMENTAL BIOLOGY

Journal of Experimental Botany
https://doi.org/10.1093/jxb/erab561 Advance Access Publication 27 December, 2021

RESEARCH PAPER

Continuous seasonal monitoring of nitrogen and water content in lettuce using a dual phenomics system

Shahar Weksler[1,2,*], Offer Rozenstein[2], and Eyal Ben Dor[1]

[1] Porter School of Environment and Earth Sciences, Faculty of Exact Sciences, Tel Aviv University, Tel Aviv 6997801, Israel
[2] Institute of Soil, Water and Environmental Sciences, Agricultural Research Organization-Volcani Institute, HaMaccabim Road 68, P.O.B 15159, Rishon LeZion 7528809, Israel

* Correspondence: weksler@mail.tau.ac.il

Received 23 August 2021; Editorial decision 21 December 2021; Accepted 23 December 2021

Editor: Michela Janni, National Research Council, Italy

Abstract

The collection and analysis of large amounts of information on a plant-by-plant basis contributes to the development of precision fertigation and may be achieved by combining remote-sensing technology with high-throughput phenotyping methods. Here, lettuce plants (*Lactuca sativa*) were grown under optimal and suboptimal nitrogen and irrigation treatments from seedlings to harvest. A Plantarray system was used to calculate and log weights, daily transpiration, and momentary transpiration rates throughout the experiment. From 15 d after planting until experiment termination, the entire array of plants was imaged hourly (from 09.00 h to 14.00 h) using a hyperspectral moving camera. Three vegetation indices were calculated from the plants' reflectance signal: red-edge chlorophyll index (RECI), photochemical reflectance index (PRI), and water index (WI), and combined treatments, physiological measurements, and vegetation indices were compared. RECI values differed significantly between nitrogen treatments from the first day of imaging, and WI values distinguished well-irrigated from drought-treated groups before detecting significant differences in daily transpiration rate. The PRI, calculated hourly during the drought-treatment phase, changed with the momentary transpiration rate. Thus, hyperspectral imaging might be used in growing facilities to detect nitrogen or water shortages in plants before their physiological response affects yields.

Keywords: chlorophyll index, hyperspectral, phenomics, PRI, reflectance, transpiration.

Introduction

Phenomics is the study of plant phenotype and its physical and biochemical qualities. It is considered a rapid method for selecting individual plants from an array based on their genome, interactions with the environment, and phenotype (Furbank, 2009; Zhao *et al.*, 2019). The use of high-throughput phenotyping systems is becoming increasingly popular in plant science (York, 2019). Recent technological advances have enabled the measurement and characterization of plant phenotypic attributes on a large scale in a rapid, non-destructive, and precise manner.

The use of remote-sensing technology in phenomics and agriculture, particularly in the hyperspectral domain, is widespread. While large-scale field research and applications rely mainly on multispectral satellite sensors or drones (Kaplan *et*

Abbreviations: DAP, days after planting; DW, dry weight;FW, fresh weight; PRI, photochemical reflectance index; PAR, photosynthetically active radiation; RECI, red-edge chlorophyll index; TR, transpiration rate; VPD, vapor pressure deficit; VI, vegetation index; WI, water index.

al., 2021), imaging spectroscopy is becoming more common as a tool in the laboratory (Eshkabilov *et al.*, 2021), field (Chapman *et al.*, 2014; Underwood *et al.*, 2017), and greenhouse (Weksler et al., 2020, 2021a, b). In addition to remote-sensing capabilities, whole-plant gravimetric systems are a key player in high-throughput phenotyping systems (Negin and Moshelion, 2017).

Lettuce (*Lactuca sativa*) has been garnering much attention in this field. It is a fast-growing plant that is harvested approximately 60–90 days after planting (DAP) under field conditions (Gallardo *et al.*, 1996; Pacumbaba and Beyl, 2011), and approximately 30 DAP in hydroponic growing systems (Donnell *et al.*, 2011). This short growing period is appealing for research because results can be obtained in a short time. Several studies using hyperspectral technology have been performed with different varieties of lettuce, for different aims. Pacumbaba and Beyl (2011) measured lettuce leaves at the end of a 90 d macronutrient-deficiency experiment using a spectrometer and found significant changes in reflectance in the red and infrared spectral regions in stressed plants. Zhou *et al.* (2018) acquired 200 hyperspectral images of lettuce leaves with five levels of water content. Using wavelet transform and partial least squares regression, they estimated leaf water content and applied the model at the pixel level to show the spatial water distribution in the leaves. Murphy *et al.* (2019) used vegetation indices (VIs) derived from hyperspectral images of leaves to quantify variations in water absorption across the different leaf components at a very high spatial resolution. They discovered that the choice of leaf component for modeling has a marked influence on the model's performance. Mo *et al.* (2015) imaged lettuce leaves with a hyperspectral camera and developed a model to distinguish discolored areas from healthy tissue. Eshkabilov *et al.* (2021) grew four lettuce cultivars with seven nitrogen (N) fertilizer treatments. They scanned freshly cut leaves using a hyperspectral camera and developed an algorithm to estimate nutrient levels in the measured leaves. Using cross-validation on 28 leaf samples, they achieved good predictive results. Although these studies show promise, they were all conducted at the scale of the leaf, mainly with cut leaves, and only once at the end of the experiment.

Early detection of drought and N deficiency can be extremely valuable in production lines. The possibility of simultaneously measuring plant physiological properties using a gravimetric system and the impact of these properties on the signal received by proximal hyperspectral sensors is a novel concept (Weksler *et al.*, 2020). Accordingly, the overarching aim of the present study was to use this combined phenomics system to investigate the detection of early symptoms of N deficiency and drought, to minimize the period between the appearance of physical symptoms in plants and their detection by the hyperspectral-sensing system. Specifically, we sought to discover how early the effects of N and drought treatments can be detected in whole plants without the need to cut their leaves, and how this compares with the plants' physiological status. We investigated these questions at the canopy (plant) level using a set of carefully selected VIs that have been shown to be correlated with changes in leaf chlorophyll and water contents. These indices were evaluated daily throughout the entire experiment and at different times of the day at key stages of the experiment.

Materials and methods

Experimental setup and plant material

The experiment was conducted in a semi-commercial greenhouse located at the Robert H. Smith Faculty of Agriculture, Food and Environment of the Hebrew University of Jerusalem in Rehovot, Israel. The temperature and relative humidity in the greenhouse were continuously monitored by the Plantarray meteorological station (Plant-Ditech Ltd, Israel). The temperature and relative humidity ranged between 13 °C and 32 °C and 28% and 92%, respectively, with low values during the night. Seventy-two lettuce seedlings (*Lactuca sativa* var. Lior) were transplanted to 3.9 litre pots. The plants were grown from 22 October to 26 November 2020.

Three different N treatments were administered to the plants: a control treatment (C), which was considered the optimal fertilization treatment (n=24 samples), a medium treatment (M), which was 70% of the control (n=24 samples), and a low treatment (L), which was 40% of the control (n=24 samples). The C, M, and L values corresponded to 70 ppm, 49 ppm, and 28 ppm N, and all other elements were administered at their optimal levels. At 25 DAP, when the plants had a daily transpiration value of approximately 250 g water, 12 plants from every treatment were subjected to progressive drought for 9 d, resulting in six treatments: the three levels of N with optimal irrigation (CW, MW, and LW), and the three levels of N with drought (CD, MD, and LD) (Fig. 1). For the drought treatment, irrigation was reduced daily to 70% of the plant's daily transpiration value on the previous day Dalal *et al.*, 2019). This method prevented rapid depletion of water during the drought treatment before the final day, on which no irrigation was provided. Then, the irrigation was returned to full capacity for 7 d to allow the plants to recover.

Phenotyping systems

A combination of two phenotyping systems was used. The first system was the Plantarray system, a high-throughput whole-plant functional phenotyping system. Individual plants were placed in the Plantarray's

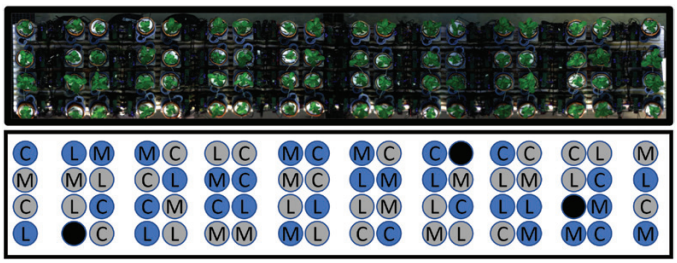

Fig. 1. Lettuce plants on the experimental table in the greenhouse, planted in the Plantarray containers (Halperin *et al.*, 2017) and connected to the logging system. The individual treatments are marked on the drawing: C, control levels of N; M, medium levels of N; L, low levels of N. Blue circles indicate plants provided with optimal irrigation throughout the experiment; gray circles indicate plants subjected to a differential progressive drought treatment initiated at 25 days after planting. Three plants that were not properly transplanted are indicated with black circles.

special load cells, which act as weighing lysimeters. Each load cell individually controlled the fertigation and logged the weight measurements. The 72 plants were randomly placed in an array on a table in the greenhouse (Fig. 1), and every 3 min, the individual weight of each plant was logged. Following the methodology described in Halperin *et al.* (2017), each pot was filled with an inert medium (quartz sand) and placed in a load cell. The drainage of the pots was restricted with a dedicated plastic container to ensure that irrigation to pot capacity was reached. Evaporation was restricted using a plastic cover with a hole in its center for the emerging plant stem, thus limiting the changes in pot weight to the effect of plant transpiration. During the night, the system selectively and automatically irrigated each pot with its selected treatment, using four drippers for even water distribution. Plant fresh weight (FW) was calculated using the Plantarray system: before planting, the load cells were loaded with pots filled with sand and irrigated to pot capacity, and these pots were weighed to determine the pre-planting pot weight. After planting, the daily plant weight was calculated as the weight after irrigation when drainage had stopped minus the pre-planting weight. Each plant's final FW was calculated as its weight on the last day of the experiment. Since the irrigation was applied only at night, and evaporation from the quartz sand was restricted, any weight change was attributed to water leaving the plant via the stomata. Thus, the plant's daily transpiration was the difference in weight between the early morning, when the plant had not transpired, and the evening, when the plant had stopped transpiring. Transpiration rate (TR) was associated with a decrease in weight throughout the daytime and was calculated by the first derivative of two consecutive weight measurements. The point at which the water content in the pot cannot sustain the demand for transpiration by drought-treated plants and stomatal conductance begins to decrease is termed the physiological critical drought point. A piecewise linear function (as described in Halperin *et al.*, 2017) was used to find the best fit between midday TR and soil water content and, consequently, the critical drought point.

On the last day of the experiment, the plants' stems were cut and the plants' shoots were placed in paper bags. The roots were carefully washed with tap water and placed in a separate paper bag. The bags were then dried in an oven for 4 d at 60 °C and the dry weight (DW) of the roots and shoots was recorded.

The second system was based on a remote-sensing system composed of a hyperspectral camera mounted on a moving platform above the plants, connected to the greenhouse's ceiling (Weksler *et al.*, 2020). The system began acquiring images at 15 DAP, when the transplanted seedlings were sufficiently large. The camera (FX10, Specim, Finland) was a push-broom sensor with a 400–1000 nm spectral range. The camera was positioned 2 m above the growing table and had 512 pixels in a row and 224 bands in the spectral range. The lightweight camera produced a signal-to-noise ratio suitable for operation under the diffuse natural light conditions in the greenhouse between 09.00 h and 14.00 h. The raw images were calibrated to radiance using a pre-calibrated gain factor produced by the camera's manufacturer and a closed shutter image (Weksler *et al.*, 2020). Then, the radiance image was transformed to reflectance using a white reference panel (99% reflectance, Spectralon, Labsphere Inc., USA) placed in the scene at each data-acquisition session. A region of interest around each plant in the image was manually selected to extract the pixels representing the plant. A binary mask was then calculated and applied to the pixels to separate the green leaves from the background. The mask was generated by calculating the slope between spectral bands (680 nm, 740 nm), and excluding the leaves' edges and shaded pixels using Otsu's filter (Weksler *et al.*, 2020). These selected pixels, representing each plant, were averaged to a mean spectral signal and smoothed using Savitzky–Golay transformation (Savitzky and Golay, 1964). The collection of mean spectral signals from each plant represented the reflectance signal of each plant at every image acquisition (Weksler *et al.*, 2020). Figure 2 summarizes the process from image acquisition to plant mean reflectance spectrum.

Hyperspectral analysis

Three different indices were carefully selected to test the effects of, and hypotheses regarding, the different treatments (Table 1). The first was the red-edge chlorophyll index (RECI) (Gitelson *et al.*, 2003), which utilizes the low sensitivity of the infrared region and the high sensitivity of the red-edge region to assess chlorophyll content. The second was the water index (WI) (Peñuelas *et al.*, 1993), which utilizes the water absorption band at ρ970 nm and a low sensitivity band outside the water absorption region at ρ900 nm. The third VI was the photochemical reflectance index (PRI) (Gamon *et al.*, 1992), which utilizes a reflectance band that is affected by physiological changes (ρ531 nm) in relation to changes in photosynthetically active radiation (PAR) and a reference band (ρ571 nm).

Three key experimental days were chosen for calculation of the indices on an hourly basis. These days represented pre-drought status (well-irrigated day; 23 DAP), the last day of drought (33 DAP), and recovery status (post-drought; 35 DAP).

Statistical analysis

ANOVA was performed to check for significant differences between the groups on an hourly or daily basis. Post hoc differences were calculated by the Tukey–Kramer test. A Welch test was used when the ANOVA assumptions of normal distribution and homogeneity of variance were not met. Post hoc comparison of differences between groups was performed using the Games–Howell post hoc test, and single pairwise comparisons were performed by using the Mann–Whitney

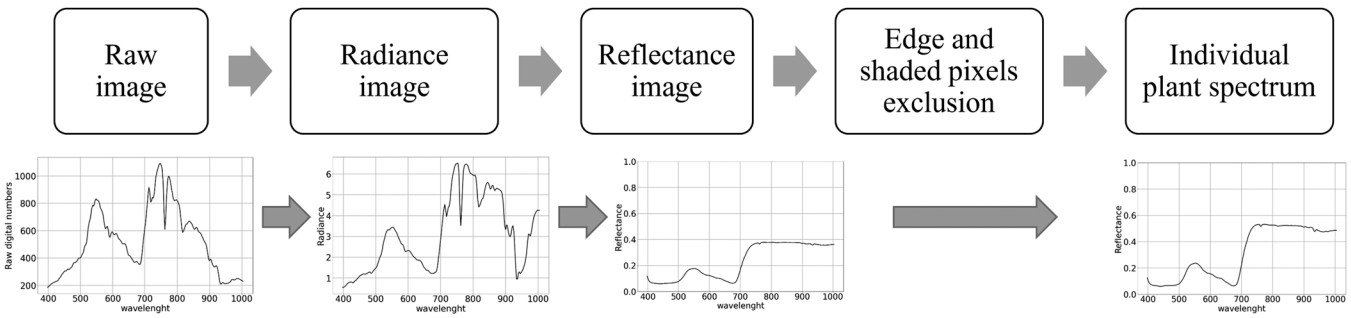

Fig. 2. Processing steps from a raw image to a plant's calibrated reflectance signal. An image was acquired every hour between 09.00 h and 14.00 h. An example of a plant's spectrum is presented for each processing step.

test. Daily outlier samples were removed using the 1.5 interquartile method (Ghasemi and Zahediasl, 2012). Using this method, the maximum number of outliers removed per group each day was found to be four, leaving a minimum of eight samples per group and a maximum of 12. All statistical differences were calculated using α=0.05 and were considered significant at $P \leq 0.05$. Statistical analysis, algorithms, and estimation were performed using Python with dedicated modules (Vallat, 2018; Terpilowski, 2019).

Following the hourly analysis, the most representative hours of the daily values were selected for the index calculations. The daily values of RECI and WI were calculated for the entire experiment and compared. In addition, the PRI was calculated explicitly on an hourly basis from 27 DAP to 30 DAP.

Results

The experiment was performed during the autumn. The atmospheric conditions throughout the imaging phase of the experiment (15–38 DAP) are presented in Fig. 3. They show typical PAR and vapor pressure deficit (VPD) values for the season. There were some cloudy and rainy periods when radiation was obscured by the clouds, which caused the VPD to drop.

The final plant FW and DW measurements are presented in Fig. 4. Significant weight differences (P<0.05) were found between the CW and LW groups (well-irrigated plants). The same significant differences were found between the plants that received the additional drought treatment from 25 DAP. Comparing the dried plants' biomass as DWs of shoots, roots, and shoots and roots together showed different behaviors. Shoot DW was significantly different between the CW and LW groups and between the CD group and both the MD and LD groups. Interestingly, the root DW of CW plants was significantly different from that of MW but not LW plants, most likely because of the relatively large standard deviation for the LW value. Root DW for CD plants was significantly different from that of plants subjected to the other two drought treatments. The DWs of shoots and roots combined tell a slightly different story: values for the CW treatment differed significantly from those of the other well-irrigated treatments. The same significant difference was calculated for the drought treatments (significant difference for CD versus MD and LD treatments).

The daily transpiration of the plants at 15–38 DAP is presented in Fig. 5. The figure also shows the TRs during each of the three representative days of the experiment. These days represent a well-irrigated day (pre-drought, 23 DAP), the last day of drought (33 DAP), and recovery (post-drought, 35 DAP). A general daily pattern that is influenced by PAR and VPD is evident, as TRs increase with an increase in PAR and VPD, and then decrease as PAR decreases (Gosa *et al.*, 2018). As well as a general pattern, a specific treatment response is apparent. On 23 DAP, the TR values are grouped by N levels, as irrigation is optimal in all cases. Later, on 33 DAP, the TR values are grouped by water availability, and on 35 DAP the grouping is similar. Furthermore, it is clear that during periods of low radiation (early in the morning and late in the afternoon), TRs are minimal, whereas they were higher during periods of moderate and high radiation (in the middle part of the day). In addition, Fig. 5 shows the direct effect of days with stormy weather (16, 27, 33, and 37 DAP) during the experiment. On those days, the temperature, PAR, and VPD were lower, and decreases in plant TRs and daily transpiration were observed. The effect of N treatment on daily transpiration among the well-irrigated plants was evident from 15 DAP, and a significant difference between the CW and LW treatment groups was observed from 17 DAP until the end of the experiment. The effect of the drought treatment on daily transpiration was evident 3 d after its initiation at 25 DAP. However, a significant difference in the daily transpiration values between well-irrigated and drought-induced plants was observed only 4 d after drought initiation (29 DAP). The physiological critical drought point was reached at 29 DAP. The different N treatments reached this point for

Table 1. The three vegetation indices used in the study

Vegetation index	Abbreviation	Formula	References
Red-edge chlorophyll index	RECI	$\frac{\sum(\rho 760 \text{ nm}:800 \text{ nm})}{\sum(\rho 690 \text{ nm}:\rho 720 \text{ nm})}$	(Gitelson *et al.*, 2003)
Water index	WI	$\frac{(\rho 900 \text{ nm})}{(\rho 970 \text{ nm})}$	(Peñuelas *et al.*, 1993)
Photochemical reflectance index	PRI	$\frac{(\rho 531 \text{ nm} - \rho 571 \text{ nm})}{(\rho 531 \text{ nm} + \rho 571 \text{ nm})}$	(Gamon *et al.*, 1992)

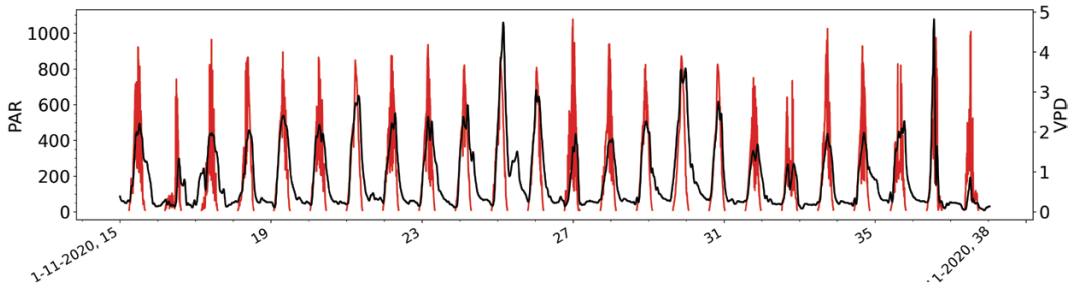

Fig. 3. Daily vapor pressure deficit (VPD, black) and photosynthetically active radiation (PAR, red) on the experimental days (days after planting) and during hyperspectral image acquisition. PAR values are shown between 06.00 h and 17.00 h when radiation was not 0.

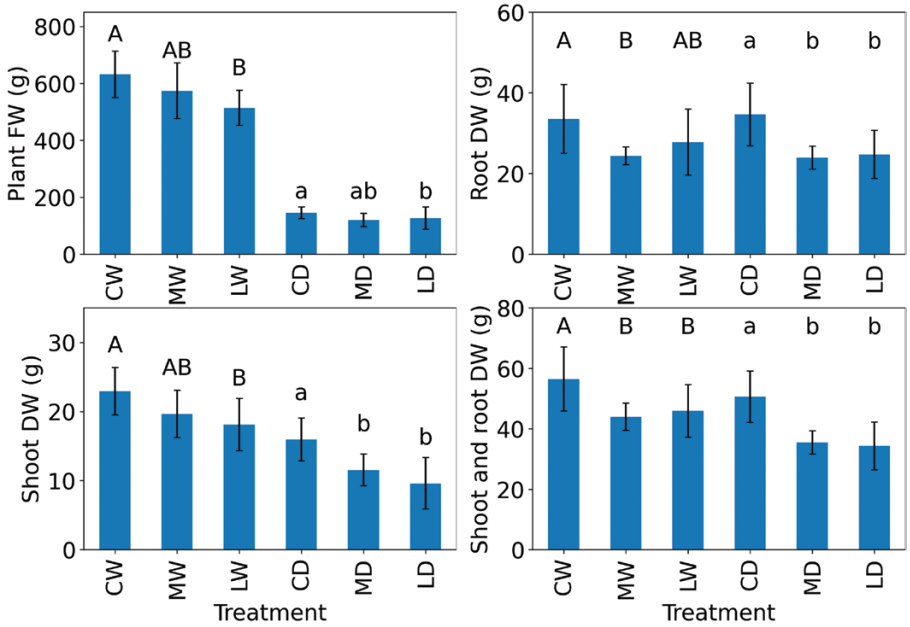

Fig. 4. The final fresh weight (FW) and dry weight (DW) measurements of the well-irrigated treatments [control N (CW), medium N (MW), and low N (LW)] and drought treatments [control N (CD), medium N (MD), and low N (LD)]. Data are presented as means ±SD. Significant differences (P<0.05) between the well-irrigated treatments are denoted with different uppercase letters, and significant differences between the drought treatments are denoted with different lowercase letters.

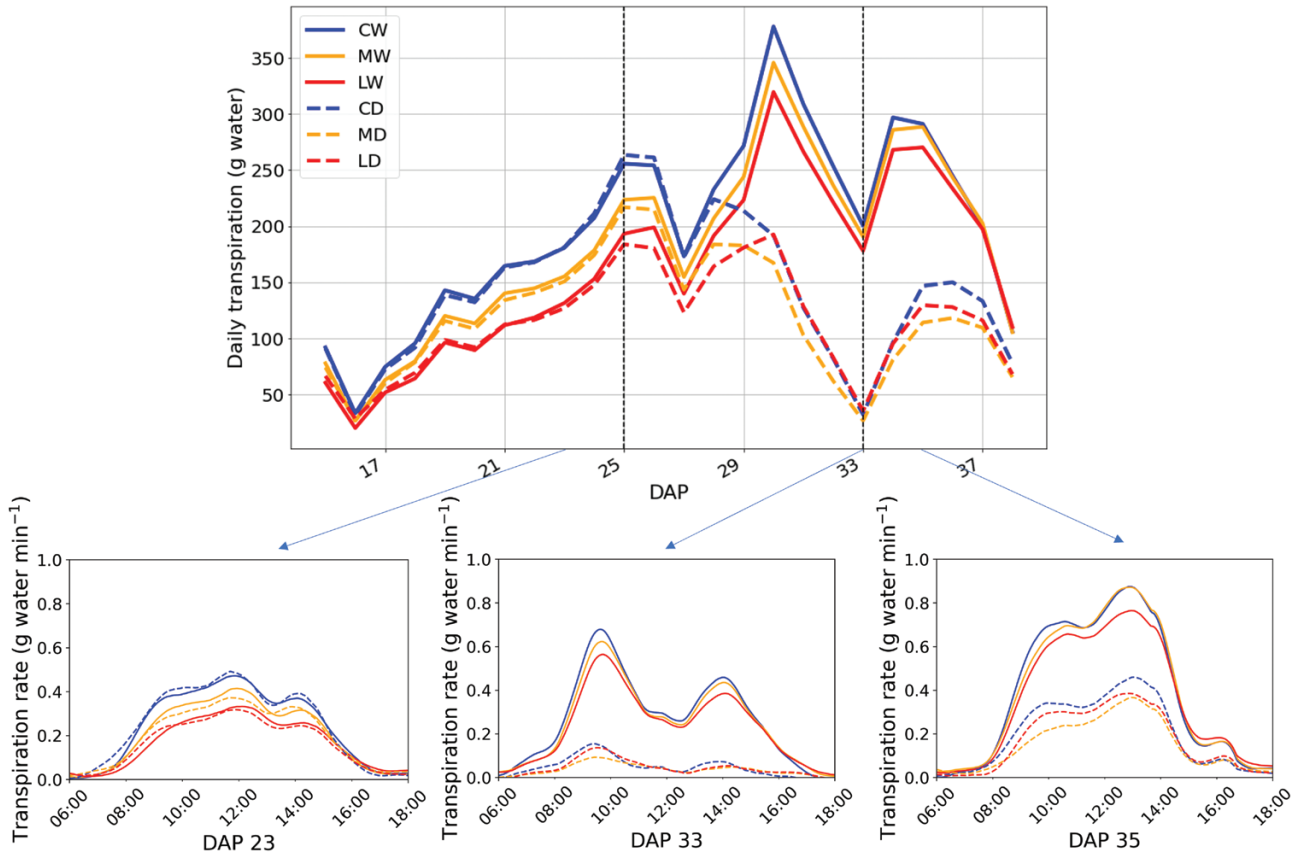

Fig. 5. Top: Daily transpiration of the treatment groups at 15–38 days after planting (DAP). The hyperspectral camera was used to acquire images on these days. Vertical dotted lines indicate the drought period. Bottom: Transpiration rates during three representative days (pre-drought, 23 DAP; drought, 33 DAP; post-drought, 35 DAP).

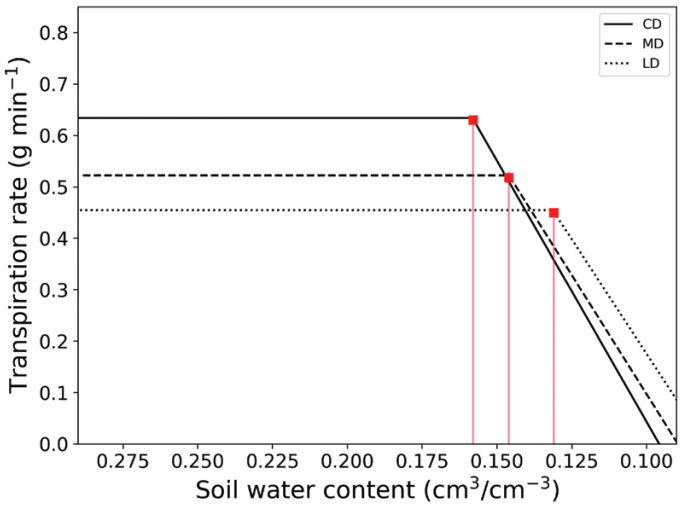

Fig. 6. Piecewise linear fit between transpiration rate and soil water content for plants subjected to drought treatment (CD, control N treatment; MD, medium N treatment). The critical drought points at which the soil water content cannot sustain the demand for transpiration were reached 4 d after the drought treatment was initiated, and are marked with red squares.

different soil water contents as the day progressed (Fig. 6). CD plants reached the critical drought point first, with a larger soil water content, followed by MD and then LD plants.

The ability to capture images at hourly intervals is displayed in Fig. 7. The three selected indices were calculated on an hourly basis over the three representative days of the experiment (pre-drought, drought, and recovery). Here, the day representing drought was 31 DAP, 2 d after significant differences in daily transpiration were found. The interaction of drought and N deficit affects chlorophyll content, leaf turgor pressure, and spongy mesophyll. Furthermore, this interaction varies dependent on rapid changes in ambient conditions in the greenhouse, such as radiation and VPD. Calculating the VIs on an hourly basis revealed the high sensitivity of this analysis, as affected by treatment and hour of the day. While a general daily pattern existed, the difference between groups varied substantially on an hourly basis and was dependent on the effect of the treatment on the plant and, consequently, on the spectra. The general pattern of PRI was maintained during the three days with a positive trend in the morning (09.00–11.00 h) followed by a negative trend around noon (12.00–13.00 h) and then a rise at 14.00 h. An hourly comparison between the treatment groups showed that during the pre-drought day, the PRI value of the CW group was significantly higher than that of the CD group at 14.00 h. In addition, during the drought period, the PRI value of the CW group was significantly higher than that of the CD group at 13.00–14.00 h. The PRI of the MW group differed significantly from that of the MD group only at 13.00 h on 35 DAP. The PRI of the LW group differed from that of the LD group at 12.00 h on 31 DAP, and at 12.00–13.00 h on 35 DAP.

The WI also showed a general pattern as the day progressed, with a positive trend during the morning, a negative trend at around noon, and variation in WI values at 14.00 h. During the pre-drought period, no significant differences in WI value were found between groups (CW versus CD, MW versus MD, and LW versus LD). Significant differences between the CW and CD groups were found during the drought period, but only during the morning (09.00–10.00 h). Post-drought, a difference in WI values between the CW and CD groups was found during the morning (09.00–11.00 h) and at 13.00 h, but this difference was not significant at 12.00 h and 14.00 h. During the pre-drought and drought periods, the WI of the MW group did not differ from that of the MD group. However, during the post-drought period, they differed significantly at 09.00 h and 12.00 h. The LW group's WI was significantly different from that of the LD group at 14.00 h on 31 DAP, and at 09.00–10.00 h and 13.00 h on 35 DAP. The WI thus seemed to be more suited to track water differences in N control plants than plants that were suffering from N deficiency.

The RECI showed the same pattern in all groups during the pre-drought day, and variations during the drought and post-drought days. The RECI of the CW group was significantly different from that of the CD group only during the pre-drought day, at 11.00 h, and a difference was observed between the LW and LD groups at 13.00 h on 35 DAP.

ANOVA between all well-irrigated groups (varying levels of N) on the three representative days showed that PRI was significantly different on 23 DAP at 12.00–14.00 h. WI was significantly different on 23 DAP at 11.00 h and on 31 DAP at 09.00 h. RECI was significantly different throughout the day on 23 DAP, and between 09.00 h and 11.00 h on 31 DAP (Fig. 8). Among the three representative days and hourly comparisons, differences between the treatments could generally be accounted for during the morning hours. In addition, during the morning hours, the plants used the available water in the pot, and the TR increased before peaking at noon. Accordingly, the daily VIs were calculated from the morning images (09.00–11.00 h) to demonstrate daily significant differences between treatments (Figs 9–12).

The daily RECI values for each of the well-irrigated treatment groups are presented in Fig. 9. The effect of the N treatment was well captured, as RECI values were significantly different between the CW and LW groups during 15–32 DAP. After this period, there was a change in trends: the RECI values of the LW and MW plants continued to increase, whereas the value for the CW group plateaued. Then, the differences between the LW and CW groups' values became significant again, but the LW group's values were higher. The RECI values for the MW treatment differed from those for both other treatments during 21–28 DAP.

The daily WI values are presented in Figs 10–12. The ability to separate well-irrigated plants from drought-treated plants was dependent on the interaction with the nutritional treatment. The CW and CD treatments showed a significant

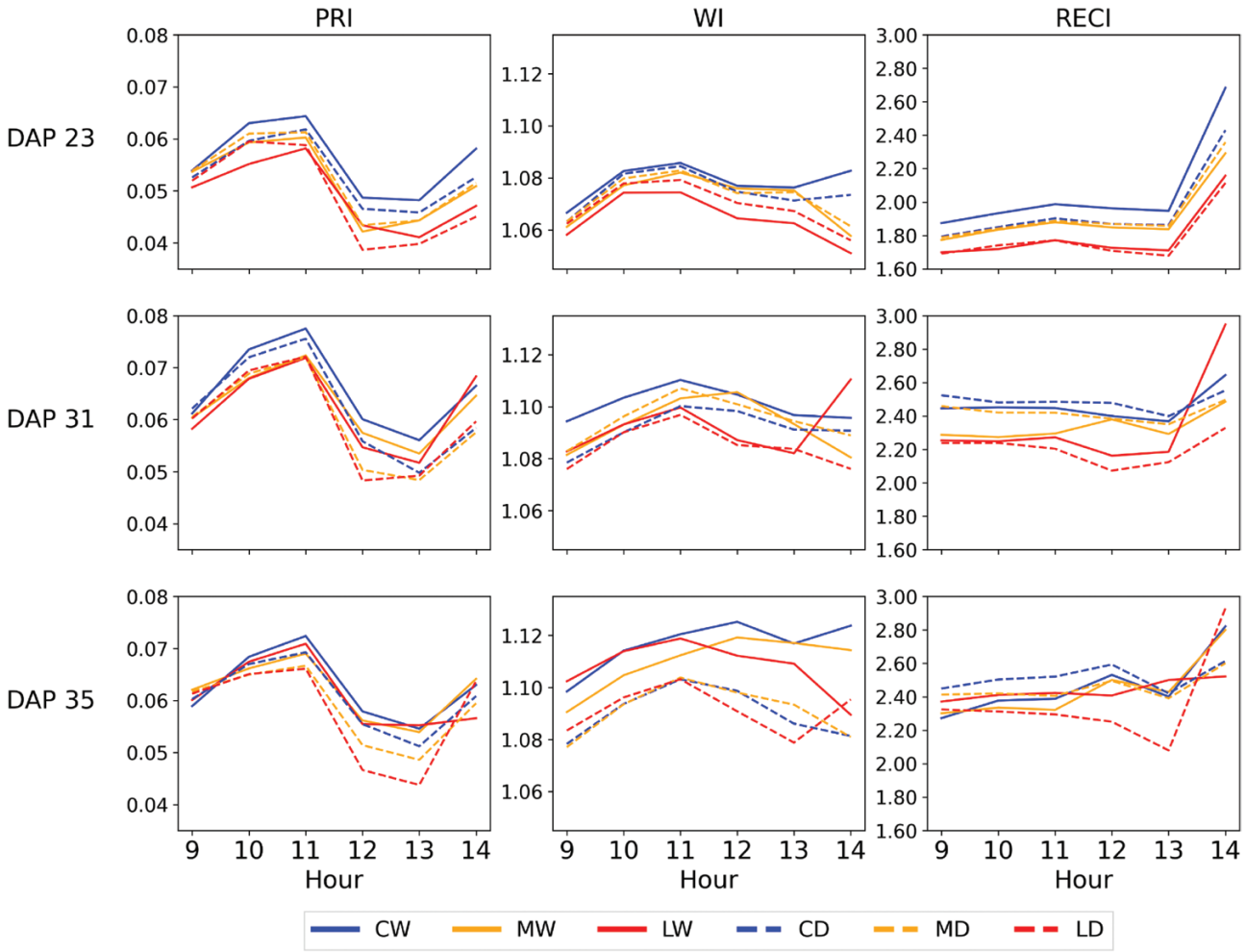

Fig. 7. Hourly values of photochemical reflectance index (PRI), water index (WI), and red-edge chlorophyll index (RECI) during three representative days: pre-drought [23 day after planting (DAP)], during drought (31 DAP), and post-drought (35 DAP). C, Control levels of N; M, medium levels of N; L, low levels of N. W, Well-irrigated treatment; D, drought treatment.

difference on 27 DAP, 2 d after the drought was initiated and 2 d before daily transpiration in the two groups of plants was significantly different (Fig. 10). The MW and MD plants presented a different behavior, with significantly different WI values occurring only once the drought treatment ended, on 34 DAP, and this difference remained until 38 DAP (Fig. 11). The LW and LD groups presented significantly different WI values during 29–38 DAP (Fig. 12).

Fig. 6 presents the critical drought point from a physical point of view. This drought point can also be seen in Fig. 13, where physical and proximal sensing are combined. During the first few days of drought treatment (27–28 DAP), the decreasing water content did not significantly affect the TRs in any N treatment group. On 29 DAP, at approximately 13.00 h, the TRs began to differ significantly between CW and CD. On the next day, as the drought progressed, this significant difference was calculated as early as 10.00 h, as the TR of CW plants continued to increase and that of CD plants reduced. Interestingly, an hourly calculation of PRI on the same days tracked this behavior almost perfectly. On 27 and 28 DAP, there were no significant differences in PRI values between the groups. Then, on 29 DAP, the PRI values differed significantly at 13.00–14.00 h, and the following day as early as 12.00 h. However, the plants that received reduced N fertilizer presented different TRs and PRI patterns. The TRs of MW and MD plants differed at approximately 13.30 h on 29 DAP and as early as 09.00 h on 30 DAP. However, the PRI values were significantly different only from 12.00 h on 30 DAP. The LW and LD TRs differed from approximately 14.00 h on 29 DAP, and from approximately 11.30 h on 30 DAP. Again, the PRI values were significantly different only on 30 DAP, from 12.00 h on. It seems that the first onset of physical drought symptoms appeared at almost the same time on 29 DAP, but varied on the next day. In contrast, the first difference in PRI between groups occurred on 29 DAP only for the optimal N group, whereas on the next day, it was exactly the same for all three groups.

Discussion

Much attention has been given to N in the remote sensing of vegetation, as have different water regimes. Combining different N treatments and drought treatments provided interesting results that supported previous findings and strengthened the use of such techniques for remote sensing of vegetation.

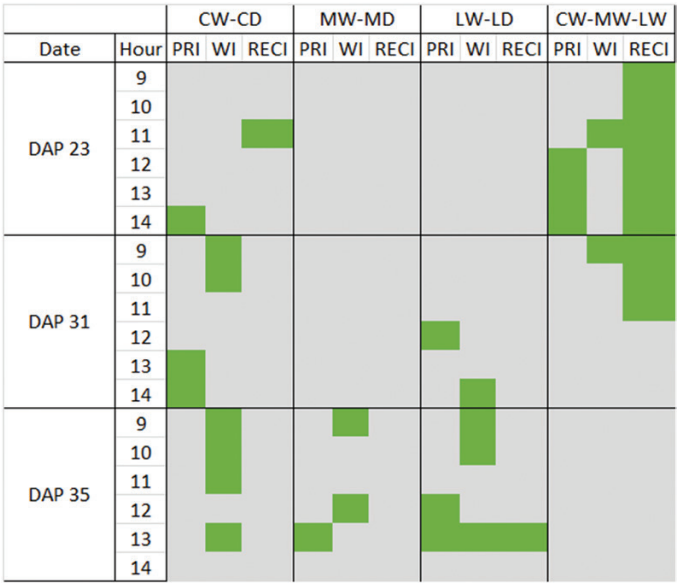

Fig. 8. Binary heat map showing significant differences between treatment groups in the calculated hourly indices. Differences were calculated between well-irrigated and drought treatments with the same N values (i.e. CW versus CD, MW versus MD, LW versus LD) and between well-irrigated treatments (CW, MW, and LW). The green color represents a significant difference ($P<0.05$) between groups at the specified hour. DAP, days after planting; PRI, photochemical reflectance index; WI, water index; RECI, red-edge chlorophyll index.

The conductance of large-scale experiments to make daily measurements without destroying plant tissue is scarce in the scientific literature. In their review, Roitsch *et al.* (2019) stated several limitations for rapid phenomics: slowness, destructiveness, laboriousness, and difficulty scaling the results from tissue to crop. The use of the combination of the Plantarray with the hyperspectral camera for research in lettuce overcame these limitations. On the other hand, indirect estimation of N using chlorophyll as a surrogate remained one of the stated limitations. However, previous experiments with this combination of systems have shown that N is not the only nutrient that can be monitored. Although potassium is difficult to estimate in the plant, since it does not create any reflectance or absorbance patterns, its quantity and influence on the plant may also be monitored during the growing season without harming the plants. In addition, momentary TRs can be estimated by a machine learning algorithm (Weksler *et al.*, 2021a). While the combination of systems has been shown to provide valuable information, it can still gain from being applied to other types of crops, which might need added attention to the image analysis methodology (e.g. plants with a different canopy or leaf morphology or senescent leaves). In such a case, it is possible that spatial information collected using a three-dimensional sensor would contribute to the analysis. Such data would likely be collected at a lower time interval than the hyperspectral and physiological data.

In the present experiment, three representative days were selected to calculate hourly differences in three VIs between the groups. The high sensitivity of this method also contributed to some hourly outliers, which constrain the identification of valuable information. While the general pattern of each index was mostly stable on the representative days, much variation was found at 14.00 h. These variations and out-of-trend results may be the result of the hourly analysis compared with

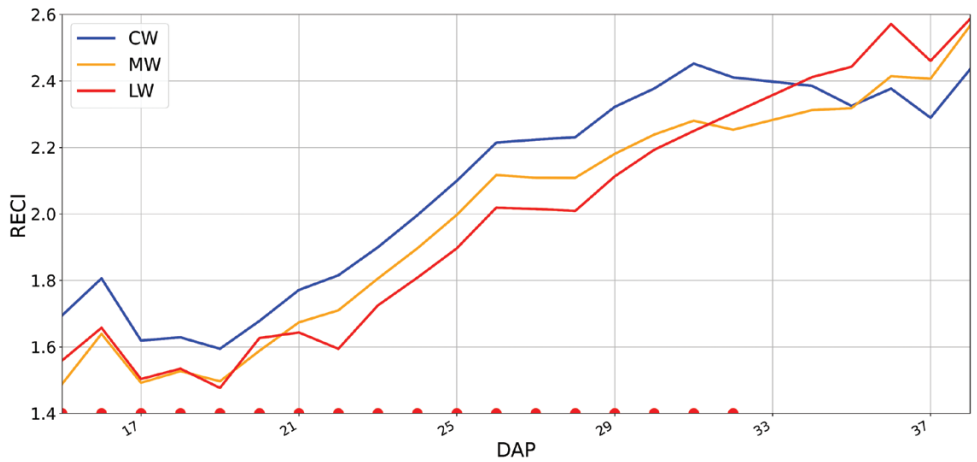

Fig. 9. Red-edge chlorophyll index (RECI) during the experiment from 15 days after planting (DAP) to 38 DAP. The index values were significantly different ($P\leq0.05$) between treatments during 15–32 DAP, indicated by red semicircles.

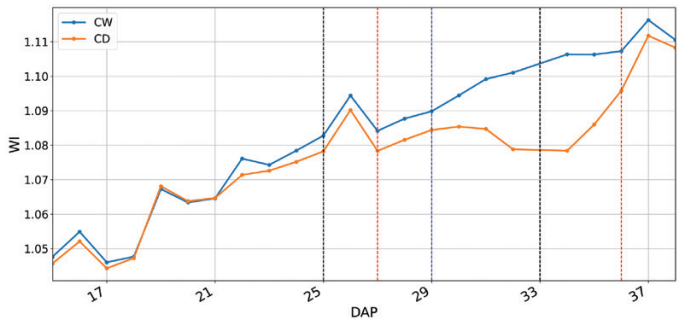

Fig. 10. Water index (WI) during the experiment from 15 days after planting (DAP) to 38 DAP. Black dashed lines represent the initiation and cessation of the drought treatment. The blue dashed line represents the day when the well-irrigated N control treatment (CW) showed a significant difference ($P \leq 0.05$) in daily transpiration compared with the drought-induced N control treatment (CD). A significant difference in WI values between the treatments was calculated for the period 27–36 DAP (red dashed lines).

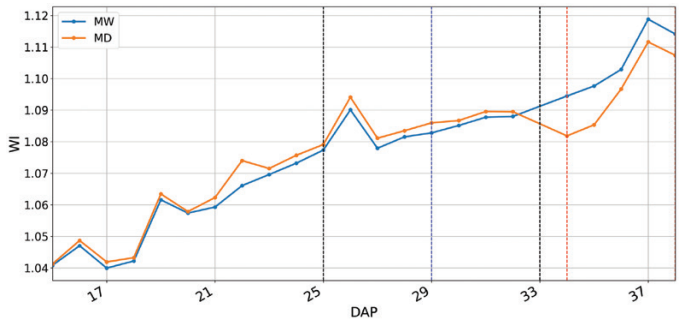

Fig. 11. Water index (WI) during the experiment from 15 days after planting (DAP) to 38 DAP. Black dashed lines represent the initiation and cessation of the drought treatment. The blue dashed line represents the day when the well-irrigated medium N treatment (MW) showed a significant difference ($P \leq 0.05$) in daily transpiration compared with the drought-induced medium N treatment (MD). A significant difference in WI values between the treatments was calculated for the period 34–38 DAP (red dashed lines).

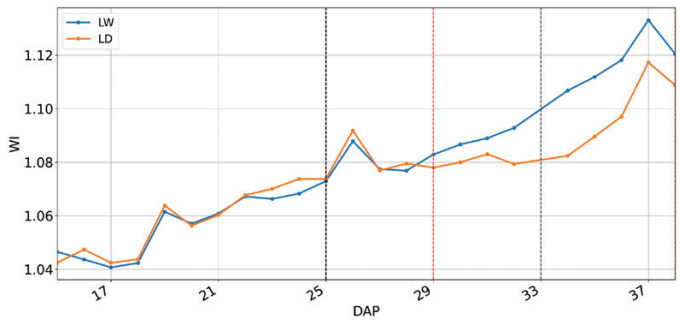

Fig. 12. Water index (WI) during the experiment from 15 days after planting (DAP) to 38 DAP. Black dashed lines represent the initiation and cessation of the drought treatment. The left red dashed line (29 DAP) represents the day on which the well-irrigated low N treatment (LW) showed significant differences ($P \leq 0.05$) in both daily transpiration and WI compared with the drought-induced low N treatment (LD). The significant difference remained until 38 DAP (right red dashed line).

daily analysis, since the mean and standard deviation are greatly affected by the sample size and extreme values. Such extreme values are probably caused by momentary alterations such as shade or the stability of the moving carriage. A significant difference was calculated between the PRI values of the control N groups (CW versus CD) during the pre-drought day, even though there was no reason for it. We therefore used the average of the morning images to represent the daily values. In addition to the morning hours, at the 13.00 h time point there were significant differences between all three indices on the post-drought day (35 DAP), especially for plants receiving the low N treatment. This is likely another expression of the different TRs found between the groups at 13.00 h (Fig. 5).

While different VIs correlated with chlorophyll are known in the literature, the RECI was shown to be very suitable and sensitive for tracking the differences between the different N treatment groups during the experiment. Significant differences in RECI values between the groups preceded the significant differences in daily transpiration calculated by the Plantarray system. This result could greatly impact commercial lines because it enables N-deficient plants to be distinguished before the deficiency has a physiological effect. Interestingly, toward the end of the experiment, the RECI values for the low N group were higher than those for the control N groups. As the plants' final FWs and DWs were significantly different (Fig. 4), the effect of the N treatments was also shown to significantly influence the plants' daily growth (Supplementary Fig. S1). However, the differences in daily growth vanished at 34 DAP, the same day on which the RECI values changed trend in the CW and LW groups. We suspect that this is because the CW plants had begun reducing their vegetative growth and were transitioning into the reproductive phase, likely induced by the stormy weather, which strongly affected the CW plants.

The effect of the medium N treatment was either not different from that of the other two treatments, or it differed from the control in terms of FW and DW. Nevertheless, the RECI values along the experiment enabled all three N treatments to be distinguished, rather than just two of them for a few days. This ability may have implications on plant yield, if N can be applied when a slight change is detected in the plant.

Calculation of the daily WI proved to be very insightful as it showed a significant difference between treatments before the daily transpiration differed, meaning that irregular irrigation can be corrected before the plant reduces its TR. However, the interaction with N-deficit treatments altered the results. Medium levels of N added much variance to the WI values, making them unusable in the drought period; low levels of N gave better WI values but were still not as good as the control N treatment. Nevertheless, it is still very promising to discover that even when plants are growing under constant N shortage, if water becomes limiting, it can be managed.

PRI is usually described as an index that changes with PAR, but using the PRI to track water changes in vegetation is not a new concept (Thenot *et al.*, 2002; Suárez et al., 2008, 2009).

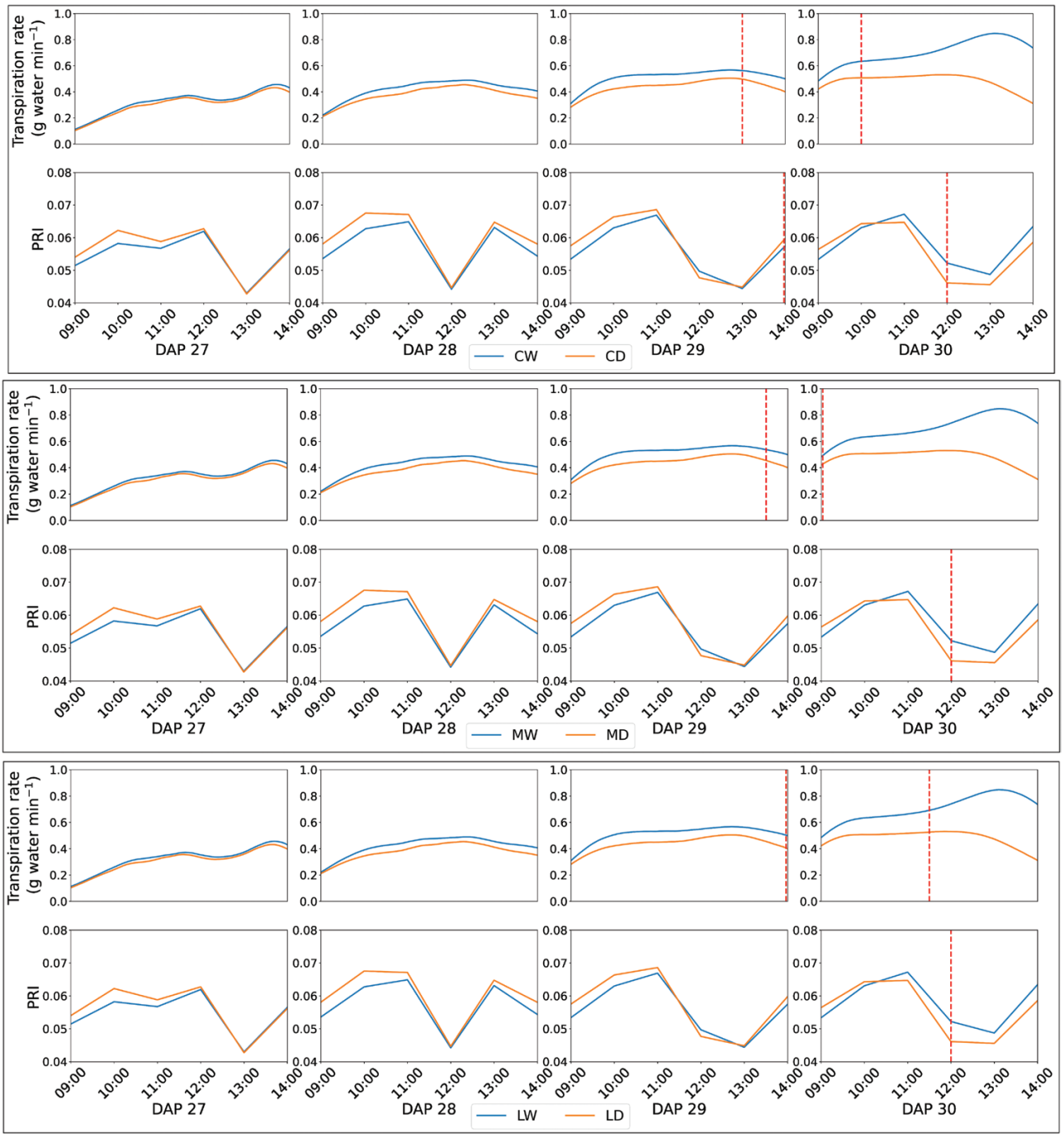

Fig. 13. Transpiration rates and photochemical reflectance index (PRI) as drought progressed for the well-irrigated N control (CW) treatment versus the drought-induced N control (CD) treatment, the well-irrigated medium N (MW) treatment versus the drought-induced medium N (MD) treatment, and the well-irrigated low N (LW) treatment versus the drought-induced low N (LD) treatment. Red dashed lines indicate the time when the treatments started to show a significant difference that lasted until the end of the daily measurements.

However, most of this previous work was conducted on simulated data. In the present study, PRI was able to track water changes in a non-destructive manner, and it almost perfectly matched the physiological behavior of the plants.

This work demonstrates the power of proximal sensing to track growing factors in lettuce and paves the way to incorporating this technology into practice. The use of hyperspectral reflectance provided early detection of the effects of the N and drought treatments. The VIs provided important information about N deficiency and water stress, and their dynamics reflected the plants' physiological responses. Suboptimal N was detected by significant differences in RECI

value, which occurred earlier than its effect on daily transpiration. Under optimal N, water limitation was detected by the WI earlier than under suboptimal N. Moreover, in this experiment, proximal sensing images provided important information during the morning hours, without the use of any artificial light source. This finding supports the potential for incorporating this technique in production lines, under natural light, and especially in phenomics research.

Supplementary data

The following supplementary data are available at *JXB* online.

Fig. S1. Daily growth of plants in the different N treatment groups.

Acknowledgements

We thank Reut Keller and Nadav Haish for their help at different stages of the research.

Author contributions

SW: formal analysis, methodology, investigation, and writing original draft; OR and EBD: supervision, funding acquisition, review, and editing.

Conflict of interest

The authors declare no conflict of interest.

Funding

This research was funded by the Israel Science Foundation (grant number 1780/18), by Israel Chemical Ltd (grant number 31010201).

Data availability

The data supporting the findings of this study are available from the corresponding author, Shahar Weksler, upon request for public research purposes and project evaluation.

References

Chapman S, Hrabar S, Chan A, Dreccer M, Holland E, Ling T, Zheng B, Jackway P, Merz T, Jimenez-Berni J. 2014. Pheno-Copter: a low-altitude, autonomous remote-sensing robotic helicopter for high-throughput field-based phenotyping. Agronomy **4**, 279–301.

Dalal A, Bourstein R, Haish N, Shenhar I, Wallach R, Moshelion M. 2019. Dynamic physiological phenotyping of drought-stressed pepper plants treated with 'productivity-enhancing' and 'survivability-enhancing' biostimulants. Frontiers in Plant Science **10**, 905.

Donnell M, Short T, Moore R, Draper C. 2011. Hydroponic Greenhouse Lettuce Enterprise Budget. Columbus: Hydroponic Program Team, Ohio State University.

Eshkabilov S, Lee A, Sun X, Lee CW, Simsek H. 2021. Hyperspectral imaging techniques for rapid detection of nutrient content of hydroponically grown lettuce cultivars. Computers and Electronics in Agriculture **181**, 105968.

Furbank RT. 2009. Plant phenomics: from gene to form and function Robert. Functional Plant Biology **36**, 1006–1015.

Gallardo M, Jackson LE, Thompson RB. 1996. Shoot and root physiological responses to localized zones of soil moisture in cultivated and wild lettuce (*Lactuca* spp.). Plant, Cell and Environment **19**, 1169–1178.

Gamon A, Peñuelas J, Field CB. 1992. A narrow-waveband spectral index that tracks diurnal changes in photosynthetic efficiency. Remote Sensing of Environment **41**, 35–44.

Ghasemi A, Zahediasl S. 2012. Normality tests for statistical analysis: a guide for non-statisticians. International Journal of Endocrinology and Metabolism **10**, 486–489.

Gitelson AA, Gritz Y, Merzlyak MN. 2003. Relationships between leaf chlorophyll content and spectral reflectance and algorithms for non-destructive chlorophyll assessment in higher plant leaves. Journal of Plant Physiology **160**, 271–282.

Gosa SC, Lupo Y, Moshelion M. 2019. Quantitative and comparative analysis of whole-plant performance for functional physiological traits phenotyping: new tools to support pre-breeding and plant stress physiology studies. Plant Science **282**, 49–59.

Halperin O, Gebremedhin A, Wallach R, Moshelion M. 2017. High-throughput physiological phenotyping and screening system for the characterization of plant–environment interactions. The Plant Journal **89**, 839–850.

Kaplan G, Fine L, Lukyanov V, Manivasagam VS, Malachy N, Tanny J, Rozenstein O. 2021. Estimating processing tomato water consumption, leaf area index, and height using Sentinel-2 and VENμS imagery. Remote Sensing **13**, 1046.

Mo C, Kim G, Lim J, Kim MS, Cho H, Cho BK. 2015. Detection of lettuce discoloration using hyperspectral reflectance imaging. Sensors **15**, 29511–29534.

Murphy RJ, Whelan B, Chlingaryan A, Sukkarieh S. 2019. Quantifying leaf-scale variations in water absorption in lettuce from hyperspectral imagery: a laboratory study with implications for measuring leaf water content in the context of precision agriculture. Precision Agriculture **20**, 767–787.

Negin B, Moshelion M. 2017. The advantages of functional phenotyping in pre-field screening for drought-tolerant crops. Functional Plant Biology **44**, 107–118.

Pacumbaba RO, Beyl CA. 2011. Changes in hyperspectral reflectance signatures of lettuce leaves in response to macronutrient deficiencies. Advances in Space Research **48**, 32–42.

Peñuelas J, Filella I, Biel C, Serrano L, Save R. 1993. The reflectance at the 950–970 nm region as an indicator of plant water status. International Journal of Remote Sensing **14**, 1887–1905.

Roitsch T, Cabrera-Bosquet L, Fournier A, Ghamkhar K, Jiménez-Berni J, Pinto F, Ober ES. 2019. Review: New sensors and data-driven approaches—a path to next generation phenomics. Plant Science **282**, 2–10.

Savitzky A, Golay MJE. 1964. Smoothing and differentiation of data by simplified least squares procedures. Analytical Chemistry **36**, 1627–1639.

Suárez L, Zarco-Tejada PJ, Berni JAJ, González-Dugo V, Fereres E. 2009. Modelling PRI for water stress detection using radiative transfer models. Remote Sensing of Environment **113**, 730–744.

Suárez L, Zarco-Tejada PJ, Sepulcre-Cantó G, Pérez-Priego O, Miller JR, Jiménez-Muñoz JC, Sobrino J. 2008. Assessing canopy PRI for water stress detection with diurnal airborne imagery. Remote Sensing of Environment **112**, 560–575.

Terpilowski MA. 2019. scikit-posthocs: pairwise multiple comparison tests in Python. Journal of Open Source Software **4**, 1169.

Thenot F, Méthy M, Winkel T. 2002. The Photochemical Reflectance Index (PRI) as a water-stress index. International Journal of Remote Sensing **23**, 5135–5139.

Underwood J, Wendel A, Schofield B, Mcmurray L, Kimber R. 2017. Efficient in-field plant phenomics for row-crops with an autonomous ground vehicle. Field Robotics **34**, 1061–1083.

Vallat R. 2018. Pingouin: statistics in Python. Journal of Open Source Software **3**, 1026.

Weksler S, Rozenstein O, Haish N, Moshelion M, Walach R, Ben-Dor E. 2020. A hyperspectral-physiological phenomics system: measuring diurnal transpiration rates and diurnal reflectance. Remote Sensing **12**, 1493.

Weksler S, Rozenstein O, Haish N, Moshelion M, Wallach R, Ben-Dor E. 2021a. Detection of potassium deficiency and momentary transpiration rate estimation at early growth stages using proximal hyperspectral imaging and extreme gradient boosting. Sensors **21**, 958.

Weksler S, Rozenstein O, Haish N, Moshelion M, Wallach R, Ben-dor E. 2021b. Pepper plants leaf spectral reflectance changes as a result of root rot damage. Remote Sensing **13**, 980.

York LM. 2019. Functional phenomics: an emerging field integrating high-throughput phenotyping, physiology, and bioinformatics. Journal of Experimental Botany **70**, 379–386.

Zhao C, Zhang Y, Du J, Guo X, Wen W, Gu S, Wang J, Fan J. 2019. Crop phenomics: current status and perspectives. Frontiers in Plant Science **10**, 714.

Zhou X, Sun J, Mao H, Wu X, Zhang X, Yang N. 2018. Visualization research of moisture content in leaf lettuce leaves based on WT-PLSR and hyperspectral imaging technology. Journal of Food Process Engineering **41**, e12647.